



Zinc uptake from ZnSO_4 (aq) and Zn-EDTA (aq) and its root-to-shoot transport in soybean plants (*Glycine max*) probed by time-resolved *in vivo* X-ray spectroscopy

Gabriel S. Montanha^a, Eduardo S. Rodrigues^a, Sara L.Z. Romeu^a, Eduardo de Almeida^a, André R. Reis^b, José Lavres Jr.^a, Hudson W. Pereira de Carvalho^{a,*}

^a University of São Paulo (USP), Center of Nuclear Energy in Agriculture (CENA), Avenida Centenário 303, 13416-000, Piracicaba, São Paulo, Brazil

^b São Paulo State University (UNESP), Rua Domingos da Costa Lopes 780, 17602-496, Tupã, São Paulo, Brazil

ARTICLE INFO

Keywords:

Zinc uptake
Micronutrient transportation *in vivo* kinetics
XRF
XANES
Chemical speciation

ABSTRACT

This study investigated the dynamic of zinc (Zn) uptake and the root-to-shoot Zn-transport when supplied as ZnSO_4 (aq) or Zn-EDTA (aq) in soybean seedlings using *in vivo* X-ray fluorescence (XRF) and X-ray absorption spectroscopy (XANES). The time-resolved X-ray fluorescence showed that plants absorbed ca. 10-fold more Zn from ZnSO_4 (aq) than from Zn-EDTA (aq). However, the uptake velocity did not influence the amount of Zn in the stem. It let furthermore appear that the plants were able to reduce the absorption of Zn from Zn-EDTA (aq) earlier than ZnSO_4 (aq). Thus, the entrance of Zn^{2+} into the roots is not necessarily accompanied by SO_4^{2-} . Regardless the source, the Zn distribution and its transport in the stem were spatially correlated to the bundles and cortex nearby the epidermal cells. Its chemical speciation showed that Zn is neither transported as ZnSO_4 (aq) nor as Zn-EDTA (aq), indicating that these compounds are retained in the roots or biotransformed on in the root-solution interface. Zn^{2+} was long-distance transported complexed by organic molecules such as histidine, malate, and citrate, and the proportion of ligands was affected by the concentration of Zn^{2+} in the stem rather than by the type of Zn source.

1. Introduction

Zinc (Zn) is a fundamental element for plant and animal nutrition. Since nutrients are exported in grains and foodstuff, intensive farming requires a proper application of Zn fertilizers to retain adequate soil fertility and therefore plants [1,2]. Furthermore, adequate applications of Zn on soybean (*Glycine max*) crops can even double the yield [3].

A reckoning estimates a production need of 10 tons ha^{-1} annual biomass to keep up 100–300 g Zn ha^{-1} [4]. However worldwide surveys on soil samples of 30 different countries shows that almost 1/3 of the assessed areas are Zn deficient [5]. In the Brazilian Cerrado (tropical Savannah), soil samples of agricultural areas presented a mean concentration of Zn lower than 1.6 mg dm^{-3} [6].

Hydrate ZnSO_4 and ZnO are the most common Zn sources, usually employed for soil and foliar fertilization [2,3,7,8], likewise Zn-EDTA is being also used as a chelated source on crop production [8,9]. It is suggested that 100–300 g Zn ha^{-1} is demanded 10 tons ha^{-1} annual biomass production [4]. Some studies performed on wheat plants

showed that Zn uptake from Zn-EDTA source was faster compared to ZnSO_4 [10], nonetheless some others claimed that complexed Zn-EDTA (aq) or insoluble ZnO uptake and translocation is lower than ZnSO_4 (aq), as the amount of Zn absorbed by roots differs according to Zn^{2+} availability and source. [11–13].

Regarding analytical strategies for Zn determination, most investigations employed atomic absorption spectroscopy [10,13] and inductively coupled plasma optical emission spectroscopy (ICP-OES) [14]. In these techniques, sample preparation is mandatory, and measurements cannot be carried out under *in vivo* or fresh conditions. Among the few studies which explored micronutrients taken up and transport in living plants [15,16], X-ray fluorescence spectroscopy (XRF) is a promising tool for *in vivo* real-time assays on the mechanism of absorption and root-to-shoot transport of micronutrients in plants [12]. Indeed, it is a well-known non-destructive analytical technique [17], which allows qualitative and quantitative elemental characterization directly on fresh plant tissues, without sample preparation [16,18,19].

* Corresponding author.

E-mail addresses: gabriel.montanha@usp.br (G.S. Montanha), eduardosr07@gmail.com (E.S. Rodrigues), sara.zachi97@gmail.com (S.L.Z. Romeu), edualm@cena.usp.br (E. de Almeida), andre.reis@unesp.br (A.R. Reis), jlavres@cena.usp.br (J. Lavres), HUDSON@cena.usp.br (H.W. Pereira de Carvalho).

<https://doi.org/10.1016/j.plantsci.2019.110370>

Received 23 July 2019; Received in revised form 2 December 2019; Accepted 4 December 2019

Available online 12 December 2019

0168-9452/ © 2019 Elsevier B.V. All rights reserved.

Although the mechanisms of ion uptake as well as root-to-shoot translocation of Zn from different Zn-sources was investigated in a myriad of plant species [16,19–21], little is known about the Zn chemical species transported by plants treated with ZnSO₄ or Zn-EDTA. In the present study, with the intention to elucidate the mechanism of Zn absorption and transport by plants, the Zn speciation was performed through synchrotron-based X-ray absorption spectroscopy (XAS) for wheat [16], common bean [19], maize [14], and soybean [22] using different Zn sources and application strategies. However, the understanding of the mechanism of Zn absorption and transport by plants is not completely clear, and thus, it needs to be better elucidated.

Employing X-ray fluorescence and X-ray absorption spectroscopy, the present study investigated the Zn transport from root-to-shoot supplied as ZnSO₄ and Zn-EDTA in soybean plants hydroponically grown. Therefore, the kinetics uptake, the spatial distribution in cross-sectioned tissues, and the chemical environment of Zn during its way up through the stem were explored.

2. Materials and methods

2.1. Cultivation assay

Soybean seeds (*Glycine max* (L.) Merrill) cv. M739 IPRO, one of the most widely cultivated variety in Brazil [23] were sowed in a moistened sandy substrate and irrigated with deionized water for fourteen days. The plants were transferred to individual plastic pots filled with 430 mL of 1:5 dilution of Hoagland modified nutrient solution (see the solution composition in Supplementary Table S1) for 7 days. Subsequently, the plant was cultivated in a nutrient solution for another 7 days (Table S1). The solution volume was daily monitored and refilled with deionized water. The plants were cultivated in a growth room at 24 ± 2 °C under 12 h-photoperiod at 250 μmol of photons m⁻² s⁻¹ using 3000 K LED lights.

The nutrient solution was spiked with ZnSO₄·7H₂O (Dinâmica, Brazil) and Zn-EDTA (Alternativa Agrícola, Brazil) yielding solutions at 100 mg L⁻¹. A control group was maintained in a nutrient solution without the Zn spike. The plants were divided into two groups of analysis, one for X-ray fluorescence spectroscopy, while another for X-ray absorption spectroscopy. The spectroscopy measurements were performed using three biological repetitions for each treatment. The solution pH was measured using the TEC-2 pHmeter (Tecnal, Brazil).

2.2. Geochem based chemical speciation

Zn chemical speciation in the nutrient solutions calculated using the Geochem-EZ software [24]. The interactions among the salts present in the hydroponic solution with either ZnSO₄ or Zn-EDTA at 100 mg L⁻¹ were assessed at pH 5.75. The distribution of Zn chemical species was presented in supplementary Table S2.

2.3. In vivo kinetics of Zn uptake

The content of Zn at the stem was monitored using a handheld XRF spectrometer (Bruker, Tracer III SD model, Germany). The X-ray beam was generated by a 4 W Rh X-ray tube operated at 40 kV and 30 μA. A primary filter (304.8 μm of Al + 25.5 μm of Ti) was added to improve the Zn signal-to-noise ratio. X-ray spectra were recorded every four hours using measuring the time of 120 s. The detection was accomplished by a silicon drift detector (SDD), with a dead time smaller than 1 %. The measurements were recorded at hypo-cotyledonary and internode region of stem. Zinc Kα intensities were normalized by the Rh Kα Compton ROI (region of interest) to correct thickness variations among the stems. The experiments were performed using three biological replicates, by each treatment.

2.4. Quantification of zinc and sulfur

Zinc and sulfur were determined in the roots and leaves through Energy Dispersive X-ray Fluorescence Spectrometry (EDXRF, Shimadzu model EDX-720, Japan). The dried samples were milled using a cryogenic grinder (Spex Sample Prep, Freezer/Mill 6870, USA). Subsequently, 100 mg of the milled samples were added in the X-ray sample cups (Spex SamplePrep no. 3577, USA) sealed with 6 μm thick polypropylene film (VHG, FPPP25-R3 USA). The samples were irradiated by a Rh X-ray tube operated at 50 kV with an auto-tunable current at a maximum of 30 % detector dead time. A 3 mm collimator and vacuum atmosphere were employed. The X-ray spectra were acquired during 200 s using a Si(Li) detector. The quantification of Zn was performed using a cellulose-based external calibration curve, while the quantification of sulfur was performed using instrumental fundamental parameters. Two standard reference materials (NIST 1515 and NIST1573a) ensured the quality of the chemical analysis. The recoveries for the S and Zn ranged from 81 to 98 % using the NIST 1515 and NIST1573a.

Zinc concentration in the stem was carried out using the emission-transmission XRF method by the microprobe X-ray fluorescence (μ-XRF, Orbis PC EDAX, USA). The stem was sectioned yielding a cylinder with a radius of 2.15 mm and a height of 11.93 mm. The fresh tissues were transferred to a sample holder covered with a 6 μm polypropylene film (VHG, FPPP25-R3, USA). The measurements were performed in three points along the stem. The samples were probed using X-rays generated by a Rh tube operated at 40 kV and 300 μA, collimated by 1 mm pin-hole. To improve the signal-to-noise ratio, a 25 μm thick Ni primary filter was used. The Zn sensitivity was determined using a Zn standard thin film at 16.2 μg cm⁻² (Serial Number 6330, Micromatter™, Canada). A metallic Zn disc was used as irradiator. This quantitative approach is described in detail elsewhere [18]. The method validation was performed using a cellulose-based Zn standard at 1000 μg g⁻¹. The recovery was 99.12%. The experiments were carried using three biological replicates, by each treatment. Analysis of variance (ANOVA) by means of Tukey test at 95% IC was performed.

2.5. X-ray fluorescence maps of stem tissue

Fresh tissues of the stems located at the same kinetic investigating area were mapped by the microprobe X-ray fluorescence (μ-XRF, Orbis PC EDAX, USA). The samples were firstly immersed in liquid nitrogen and transversely cut using a stainless-steel razor blade. Then, they were placed in a sample holder covered with a 6 μm polypropylene film (Spex Sample Prep, no. 3520, USA) and immediately investigated by μ-XRF. The X-rays were generated by a Rh anode operated at 40 kV and 900 μA, and a 25 μm Ti primary filter was selected. The sample was interrogated using 30 μm polycapillary optic during 1 s per point, and the maps were obtained by interpolating 25 × 32 pixels. The X-ray fluorescence was detected by an SDD, and the dead time was smaller than 10%.

2.6. XAS chemical speciation

Each substance has its own spectral signature. Basically, the XANES (X-ray absorption near edge structure) evaluated the edge region (E₀) and region below E₀ regarding the analyte X-ray absorption spectrum. X-ray absorption spectroscopy allows to identify the chemical environment of elements. It is usually divided into two spectral regions named XANES (X-ray absorption near edge structure) and EXAFS (extended X-ray absorption fine structure). Since XANES comprises a short energy range, the measurements are faster and the signal-to-noise ratio is much higher than in the EXAFS part of the spectrum. The XANES spectrum is a fingerprint of the chemical environment of Zn. The spectrum mixture can be decomposed through a linear combination analysis affording the fraction determination of each component [25].

This technique affords the electronic and chemical states evaluation of the analyte [26].

On this scenario, Zinc speciation by XANES was performed at the X-ray absorption beamline XAFS2 at the 1.37 GeV Brazilian Synchrotron Light Laboratory (LNLS). The X-ray beam was monochromatized by a Si (111) double crystal and a KB mirror system focused a nearly $500 \times 250 \mu\text{m}^2$ beam on the sample, additional details of the beamline are described elsewhere [27]. The XANES spectra for plant stems and liquid samples were acquired in fluorescence geometry (Canberra 15 element Ge solid-state) and in transmission mode (ion chambers), respectively.

XANES spectra were collected at three locations in the stem of living plants, right above the cotyledonal leaves, as shown in Supplementary Fig. S1. Each XANES spectrum required six minutes to be recorded.

The energy of the XANES spectra was calibrated using a metallic Zn foil, normalized and subjected to linear combination fitting (LCF) from -10 to 70 eV, relatively to the edge threshold using the Athena software of the IFEFFIT package [28]. The reference compounds ($\text{Zn-malate}_{(\text{aq})}$, $\text{Zn-citrate}_{(\text{aq})}$, $\text{ZnSO}_4_{(\text{aq})}$, and $\text{Zn-EDTA}_{(\text{aq})}$) were prepared at 2000 mg L^{-1} and the pH adjusted to 5. Only Zn-histidine was measured as pelletized solid, prepared as described by Savassa et al. [18].

3. Results

3.1. Characterization of Zn in solution

Fig. 1A presents the reference XANES spectra of aqueous solutions of $\text{ZnSO}_4_{(\text{aq})}$ and $\text{Zn-EDTA}_{(\text{aq})}$. The spectral features reveal differences in chemical environment between them. After 48 h under nutrient solution and root influence, both compounds presented modified white-line intensity compared to pristine ones (Fig. 1B). For the sake of clarity, the whiteline means the maximum intensity of the $\mu(E)$ in the X-ray absorption spectrum, roughly the whiteline for Zn K edge is at 9.66 keV. However, the changes on $\text{ZnSO}_4_{(\text{aq})}$ were more evident. The LCF in Fig. 1C shows that 17% of Zn^{2+} from $\text{ZnSO}_4_{(\text{aq})}$ presented a chemical environment like $\text{Zn-EDTA}_{(\text{aq})}$ after 48 h in nutrient solution.

3.2. Root to shoot uptake of $\text{ZnSO}_4_{(\text{aq})}$ x $\text{Zn-EDTA}_{(\text{aq})}$

Fig. 2A shows the experimental setup used for the *in vivo* monitoring of Zn uptake, while Fig. 2B presents the average intensity of Zn in the stem of soybean plants. Since the X-ray fluorescence yield depends on the number of atoms within the irradiated volume, the Zn intensity is directly proportional to the Zn concentration. However, transforming the number of counts in concentration, *i.e.*, mg Zn kg^{-1} of tissue, requires a calibration curve that is out of the scope of the present study. The number of counts showed that after 48 h exposure, the Zn in the stem treated with $\text{ZnSO}_4_{(\text{aq})}$ was *ca.* 10-fold higher than the ones which were treated with $\text{Zn-EDTA}_{(\text{aq})}$ and 50-fold higher than the control plant. Fig. S2 shows the data acquired for each biological repetition.

Fig. 2. (A) Setup for *in vivo* monitoring of Zn uptake; (B) average ($n = 3$) number of XRF counts of Zn in the stem as a function of time for control, $\text{ZnSO}_4_{(\text{aq})}$ and $\text{Zn-EDTA}_{(\text{aq})}$ treatments. XRF allowed tracing the Zn in the stem of living plants, the soybean plants treated with $\text{ZnSO}_4_{(\text{aq})}$ accumulated more Zn than those exposed to $\text{Zn-EDTA}_{(\text{aq})}$.

Fig. 3 shows that the uptake of Zn can be fitted using a sigmoidal logistic function, as shown in Eq. (1).

$$\text{Zn intensity} = \frac{L}{(1 + e^{-k(x-x_m)})} \quad (1)$$

where,

L = Zn maximum intensity

x_m = Zn midpoint intensity

k = logistic growth rate (uptake velocity)

x = time (h)

Table 1 presents the concentration of Zn in the roots and leaves of

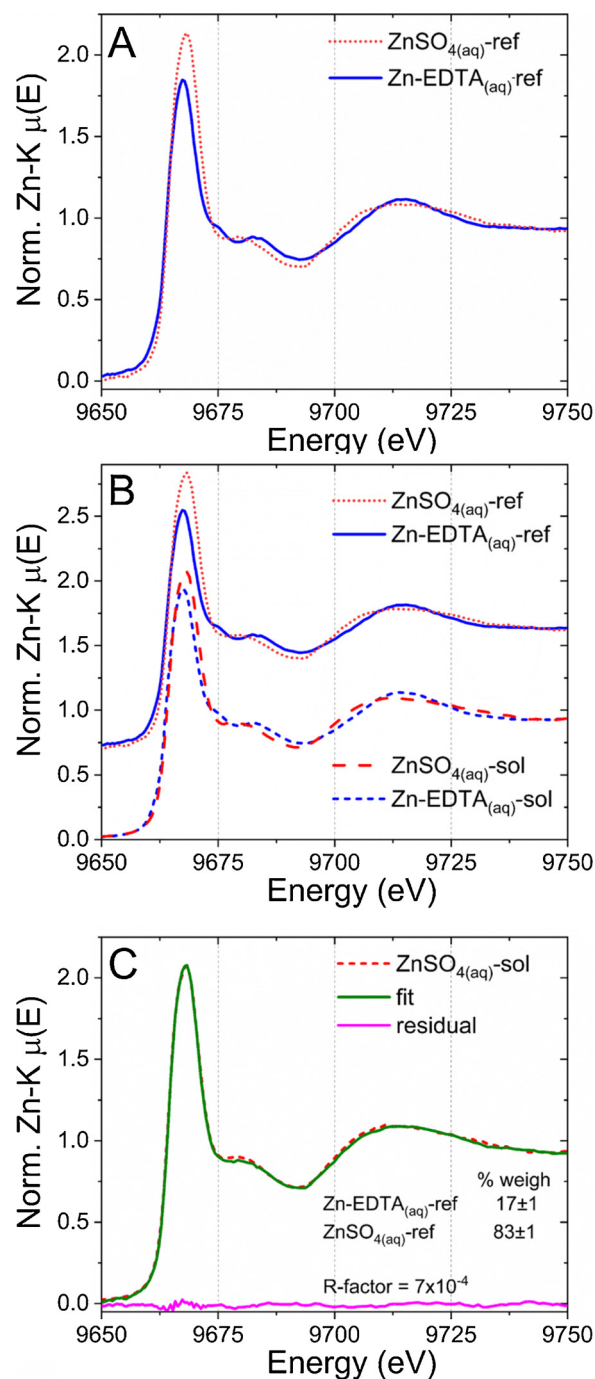


Fig. 1. (A) Reference solutions (ref) at 2000 mg L^{-1} for $\text{ZnSO}_4_{(\text{aq})}$ ($\text{pH} = 3.9 \pm 0.1$) and $\text{Zn-EDTA}_{(\text{aq})}$ ($\text{pH} = 6.9 \pm 0.1$); (B) Nutrient solutions (sol) at 100 mg L^{-1} for $\text{ZnSO}_4_{(\text{aq})}$ -sol ($\text{pH} = 5.5 \pm 0.5$) and $\text{Zn-EDTA}_{(\text{aq})}$ -sol ($\text{pH} = 6.7 \pm 0.2$) after 48 h root contact and reference compounds (ref); (C) Linear combination fitting of $\text{ZnSO}_4_{(\text{aq})}$ -sol under nutrient solution.

soybean plants. The concentration of Zn in roots increased by a factor of *ca.* 32 and 3 compared to the control, for the plants exposed to $\text{ZnSO}_4_{(\text{aq})}$ and $\text{Zn-EDTA}_{(\text{aq})}$, respectively. The concentration of S increased for the $\text{ZnSO}_4_{(\text{aq})}$ treatment by a factor less than 2.

3.3. Spatial distribution of Zn in the stem

Fig. 4 shows the spatial distribution of Zn and the intensity of Compton scattering at the cross-sections of the stem. The analyses were performed in the same region irradiated in Fig. 2A. In agreement with

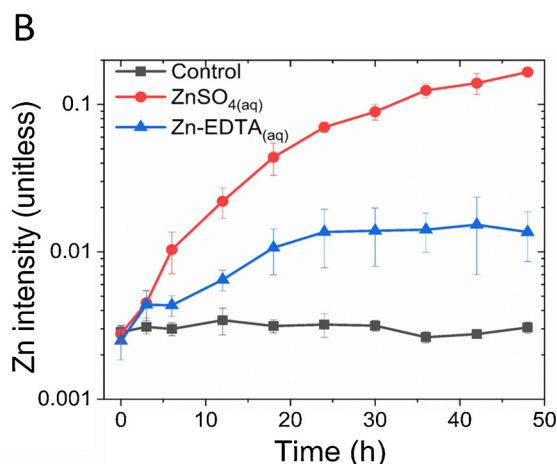


Fig. 2. (A) Setup for *in vivo* monitoring of Zn uptake; (B) average ($n = 3$) number of XRF counts of Zn in the stem as a function of time for control, ZnSO_4 (aq) and Zn-EDTA (aq) treatments. XRF allowed tracing the Zn in the stem of living plants, the soybean plants treated with ZnSO_4 (aq) accumulated more Zn than those exposed to Zn-EDTA (aq).

the kinetic data, one can note that Zn intensity was higher in Fig. 4A, which corresponds to the plant exposed to ZnSO_4 (aq). Regardless of the treatment, Zn is mostly concentrated at primary and secondary xylem vessels of soybean seedlings.

3.4. Chemical speciation

To verify whether X-ray exposure induced any spectral changes in XANES analysis, *i.e.* radiation damage, a series of individual XANES spectra were recorded at the different stem positions, and then another set of subsequent spectra obtained at the same stem position as shown in Fig. S1. Each of these positions was labeled as PA, PB, and PC (see supplementary Fig. S1). Fig. 5 presents the XANES spectra recorded at these positions. The radiation damage was characterized by the reduction of the white line intensity. Radiation damage occurred from the third spectra recorded at the same point, *i.e.*, after at least 12–24 min of beam exposure. One can observe it in four out of six plants (Fig. 5B, D, E, and F), thus it suggests that biological variability might influence this phenomenon.

Hence, to avoid artifacts and improve the spectral signal-to-noise ratio, we averaged only the first XANES spectrum recorded at each position of the stem. Fig. 6A and B overlay the spectra recorded at three different plants and the reference Zn compounds spiked in the nutrient solution. The spectral comparison indicated that inside the plant, Zn is neither transported as ZnSO_4 (aq) nor as Zn-EDTA (aq). Additionally, Fig. 6A (ZnSO_4 (aq) treatment) shows slight spectral differences between plants subjected to the same treatment, while the shape of XANES spectra shown Fig. 6B (Zn-EDTA (aq) treatment) is more consistent.

In order to estimate the chemical environment of Zn in the plants, the spectra were subjected to LCF using the reference compounds shown in Fig. 6C. As shown in Fig. S3A reference Zn-malate (aq) and Zn-EDTA (aq) presented close spectral features. Consequently, they could

Table 1

Concentration of zinc and sulfur in the roots and stem of soybean (*Glycine max*). Values followed by the same letters does not present statistical difference according to Tukey test with $p = 5$.

| Roots | Zn concentration (mg kg ⁻¹) | S concentration (g kg ⁻¹) | S/Zn molar ratio |
|-----------------------|---|---------------------------------------|------------------------|
| Control | 50 ± 40 ^a | 3.5 ± 0.5 ^a | 200 ± 130 ^a |
| ZnSO_4 (aq) | 1580 ± 30 ^b | 5.4 ± 0.11 ^a | 6.9 ± 0.3 ^b |
| Zn-EDTA (aq) | 140 ± 40 ^a | 4.3 ± 0.4 ^a | 70 ± 30 ^{ab} |
| Leaves | | | |
| Control | 37 ± 5 ^a | 2.9 ± 0.6 ^a | 160 ± 30 ^a |
| ZnSO_4 (aq) | 320 ± 80 ^b | 3.8 ± 0.4 ^b | 25 ± 3 ^b |
| Zn-EDTA (aq) | 150 ± 20 ^c | 3.1 ± 0.3 ^a | 41 ± 4 ^b |

replace each other in the LCF. Table 2 presents the obtained percent fractions using two approaches, *i.e.*, using either Zn-malate (aq) or Zn-EDTA (aq), the fitted curves and residues are presented in Fig. S4 and S5, respectively. The LCF results yielded slightly lower disagreement factor (R-factor) when Zn-EDTA (aq) was used instead of Zn-malate (aq). One exception was observed for Plant3 exposed to the ZnSO_4 (aq).

The spectra recorded at the stem of plants exposed to Zn-EDTA (aq) required four components in the LCF, whilst three components were enough to adjust the spectra obtained from plants treated with ZnSO_4 (aq). The fourth component, above-mentioned was Zn-citrate (aq). Fig. S3B shows that among the reference compounds, Zn-citrate (aq) presented the highest whiteline, this feature was responsible for the fitting improvement in the plants treated with Zn-EDTA (aq). The Plant3 exposed to the ZnSO_4 (aq) also exhibits small R-factor when Zn-citrate (aq) was added to the LCF.

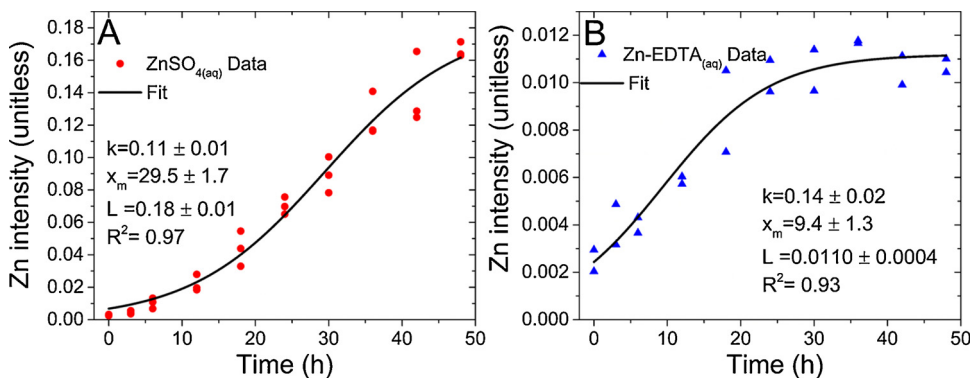


Fig. 3. Experimental data and fitted Zn intensity curves for plants exposed to (A) ZnSO_4 (aq) ($n = 3$) and (B) Zn-EDTA (aq) ($n = 2$) at 100 mg L^{-1} . The fitted curves were obtained using Eq. (1). The Zn intensity variation over time was similar for both treatments. However, the inflection for Zn-EDTA (aq) occurred earlier than ZnSO_4 (aq).

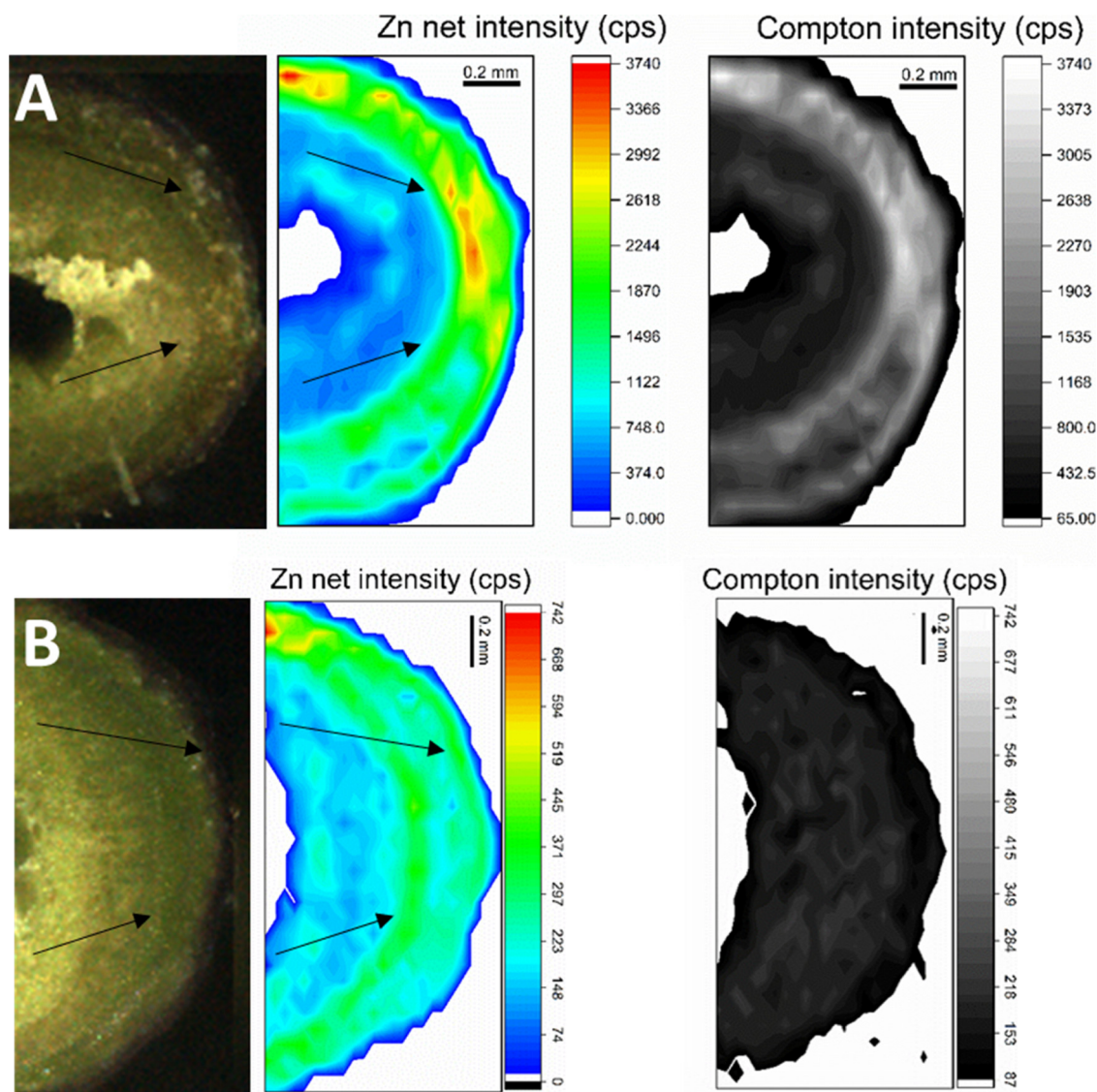


Fig. 4. Stem photograph (left side), X-ray fluorescence chemical images revealing the spatial distribution of Zn (middle) and Compton intensity (right side) in the stem of soybean plants (*Glycine max*) exposed to 100 mg L^{-1} (A) $\text{ZnSO}_{4(\text{aq})}$ and (B) $\text{Zn-EDTA}_{(\text{aq})}$. Note that the higher Zn intensities are concentrated at primary and secondary xylem vessels of soybean seedlings, as shown by the arrows.

4. Discussion

Observable changes in Fig. 1 may be a consequence of pH or reaction between Zn^{2+} and anions found in the nutrient solution. According to a calculation performed by Geochem, in a pristine nutrient solution 5.8 % of Zn^{2+} is chelated with EDTA, and 79 % is found as $\text{Zn}^{2+}_{(\text{aq})}$ in the nutrient solution, while the remaining is precipitated with PO_4^{2-} and complexed to other anions. In the case of a pristine nutrient solution (prior to zinc spike), the EDTA was added together with Fe^{2+} . The LCF results shown in Fig. 1C are in close agreement with the calculated value. On the other hand, the calculation showed that when $\text{Zn-EDTA}_{(\text{aq})}$ is added to the nutrient solution, 99.96% of Zn remains chelated by EDTA.

The imbalance between the content of Zn and S in roots showed that the absorption of $\text{Zn}^{2+}_{(\text{aq})}$ does not take place together with $\text{SO}_{4(\text{aq})}^{2-}$. Therefore, the maintenance of electrical neutrality within roots might rely on the efflux of cations such as H^+ [29]. The concentration of Zn in the plant roots treated with $\text{ZnSO}_{4(\text{aq})}$ was 10-fold higher than $\text{Zn-EDTA}_{(\text{aq})}$. This order of magnitude agrees with the XRF counts measured in the stem.

Zn moves through apoplastic and symplastic pathways in the roots

[30–32]. The admission of Zn in root apoplast takes place through a combination of mass transport, and diffusion from the nutrient solution [33], the coefficients for $\text{Zn}^{2+}_{(\text{aq})}$ and $\text{Zn-EDTA}_{(\text{aq})}$ are 125.4 and $58.2 \cdot 10^{-6} \text{ cm}^2 \text{ s}^{-1}$ [34], respectively. Therefore, the ionic root uptake by gradient diffusion is expected to be lower for $\text{Zn-EDTA}_{(\text{aq})}$. Additionally, at the pH provided by the nutrient solution (5.5–6.7), the $\text{Zn-EDTA}_{(\text{aq})}$ complex is predominantly negatively charged as $\text{Zn[EDTA]}_{(\text{aq})}^{2-}$ [35]. Due to its charge, the cell membrane presents more affinity to cations than anions [36]. Another important point regards the high stability constant of $\text{Zn-EDTA}_{(\text{aq})}$ ($\log K = 16.5$), which would impose a longer time to release Zn to the membrane transporters compared to $\text{Zn}^{2+}_{(\text{aq})}$. Hence, the limiting factor controlling the content of Zn in the stem is the entrance of Zn in the root apoplast and symplast rather than the loading of Zn from roots into the primary and secondary xylem or the transport along the xylem itself.

Zinc content in the stem experienced an exponential increase followed by saturation. According to Fig. 3, the uptake velocity, expressed by the logistic growth factor (k) in Eq1, was virtually the same for both treatments. However, the midpoint of sigmoid, i.e., the x_m factor of Eq1 points out the moment at which the growth rate starts decreasing, was achieved faster for $\text{Zn-EDTA}_{(\text{aq})}$ ($9.4 \pm 1.3 \text{ h}$) compared to $\text{ZnSO}_{4(\text{aq})}$

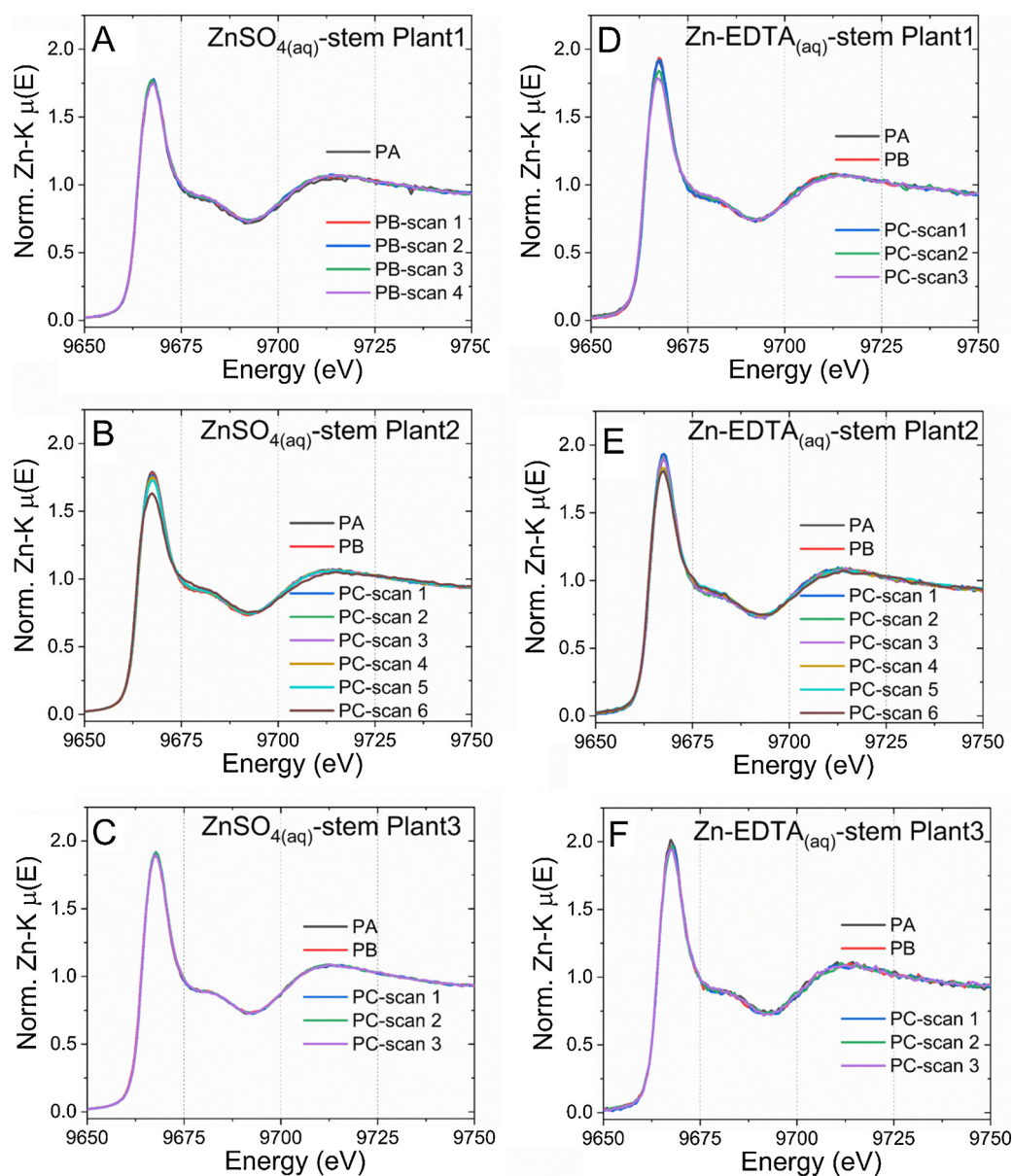


Fig. 5. Zn-K XANES spectra recorded at the stem of soybean (*Glycine max*) plants to evaluate the radiation damage caused during *in vivo* measurements. From A–C the plants were exposed to $\text{ZnSO}_{4(\text{aq})}$, and from D–F the plants were exposed to $\text{Zn-EDTA}_{(\text{aq})}$, both at 100 mg L^{-1} for 48 h. PA, PB, and PC correspond to the position of the stem at which the spectra were recorded.

(29.5 ± 1.7 h). This delay should be consequence of the amount of Zn^{2+} available at the root-solution interface (Fig. 1C), such high concentration of complexed $\text{ZnSO}_{4(\text{aq})}$ might have delayed the homeostatic response. Because of the high concentration provided by the $\text{ZnSO}_{4(\text{aq})}$, the root-to-shoot dilution effect was more evident for plants exposed to $\text{Zn-EDTA}_{(\text{aq})}$. The stem seems to act as a buffer storing the Zn excess protecting the photosynthetic apparatus in soybean leaves. Despite the increase of Zn concentration in the leaves (Table 1), no symptoms of intoxication such as stain, spots, or leaf wilting were observed past 48 h exposure.

A critical step in chemical speciation of biological samples regards the changes in the chemical environment of target elements caused by sample preparation, storage, and X-ray radiation. Chemical fixation, such as the processes used to maintain the tissue integrity, increase the risk to modify the chemical neighborhood the elements of interest.

A preservation method widely accepted consist of cryofixation by flash freezing the samples in supercooled isopentane [37]. Then, the samples can be freeze-dried or measured hydrated under the stream of a

cryojet [25]. Other possibility consists in the direct analysis under *in vivo* or fresh conditions. In any case, one must deal with potential damage caused by the radiation. *In vivo* analysis brings the advantage of measuring the same individual, hence isolating genetics and environmental factors. Reducing exposure time, or measurements at multiple locations, are strategies to circumvent radiation damage. These approaches were proposed during *in vivo* chemical speciation of thallium in *Iberis intermedia* [38].

In XRF, radiation damage may alter the spatial distribution of elements, whereas for XAS artifacts are related to changes in the chemical environment, especially *via* redox reactions. In both cases, radiation damage depends on X-ray dose, *i.e.*, exposure time and power. Supplementary Fig. S6A shows that an X-ray beam provided by focusing optics can alter the chemical composition of a soybean stem while the collimator used in the handheld equipment did not (See the supplementary material for experimental details). In this assay, the focused X-ray beam presented a flux density at least 2000-fold higher than that provided by the handheld equipment.

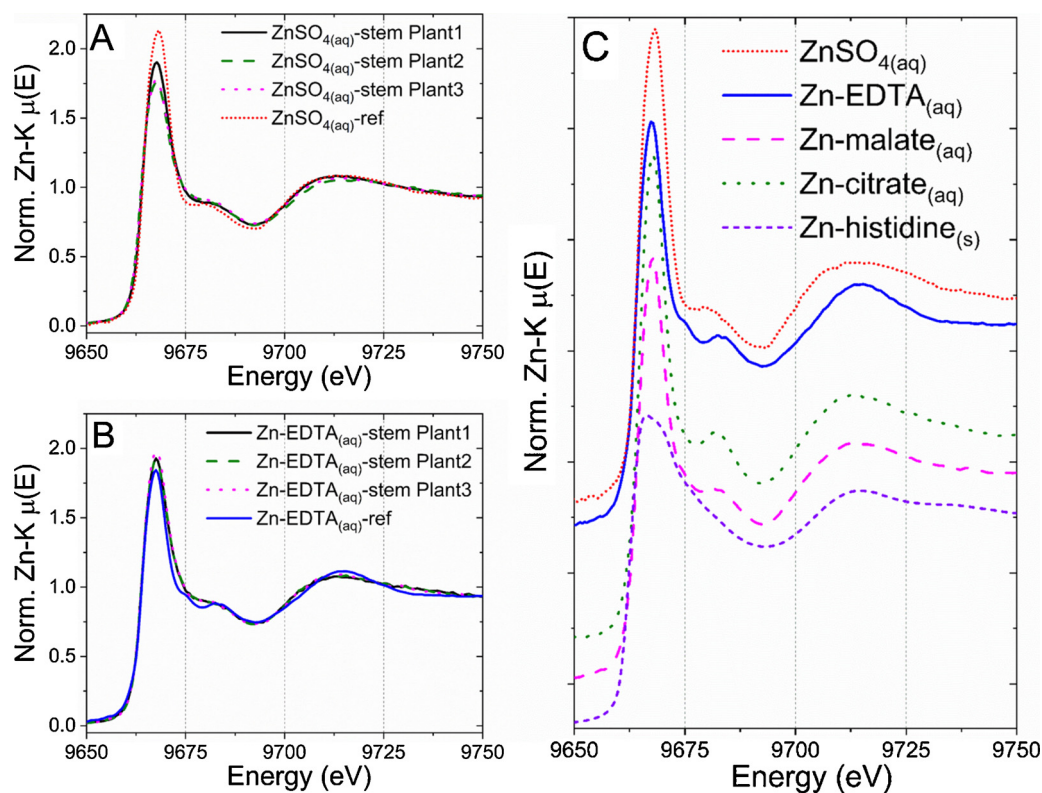


Fig. 6. Zn-K merged XANES spectra recorded under *in vivo* conditions at the stem of soybean (*Glycine max*) plants hydroponically exposed to (A) Zn-EDTA_(aq) and (B) ZnSO_{4(aq)}; (C) presents the spectra recorded for reference compounds used in the linear combination fitting.

Table 2

Linear combination fittings for the XANES spectra recorded at the stem of soybean (*Glycine max*) exposed to 100 mg L⁻¹ of ZnSO_{4(aq)} and Zn-EDTA_(aq).

| Spectra recorded at the stem | Composition (%) | | | | | R-factor x10 ⁻³ |
|--|-------------------------|---------------------------|-----------------------|-----------------------------|----------------------------|-------------------------------|
| | Zn-EDTA _(aq) | Zn-malate _(aq) | ZnSO _{4(aq)} | Zn-histidine _(s) | Zn-citrate _(aq) | |
| Using Zn-malate_(aq) in LCF | | | | | | |
| Zn-EDTA _(aq) -stem Plant1 | | 17 ± 5 | 27 ± 5 | 29 ± 9 | 27 ± 5 | 1.4 |
| Zn-EDTA _(aq) -stem Plant2 | | 13 ± 5 | 29 ± 5 | 30 ± 10 | 28 ± 5 | 1.6 |
| Zn-EDTA _(aq) -stem Plant3 | | 0 | 32 ± 6 | 26 ± 11 | 42 ± 6 | 2.0 |
| ZnSO _{4(aq)} -stem Plant1 | | 44 ± 4 | 20 ± 3 | 36 ± 5 | | 1.1 |
| ZnSO _{4(aq)} -stem Plant2 | | 37 ± 3 | 26 ± 2 | 37 ± 4 | | 0.6 |
| ZnSO _{4(aq)} -stem Plant3 | | 31 ± 3 | 46 ± 2 | 24 ± 4 | | 0.6 |
| ZnSO _{4(aq)} -stem Plant3 | | | 27 ± 4 | 42 ± 3 | 8 ± 3 | 0.6 |
| Using Zn-EDTA_(aq) in LCF | | | | | | |
| Zn-EDTA _(aq) -stem Plant1 | 20 ± 3 | | 32 ± 4 | 25 ± 15 | 23 ± 5 | 1.1 |
| Zn-EDTA _(aq) -stem Plant2 | 17 ± 4 | | 33 ± 4 | 27 ± 15 | 23 ± 5 | 1.4 |
| Zn-EDTA _(aq) -stem Plant3 | 8 ± 4 | | 32 ± 5 | 23 ± 16 | 37 ± 6 | 1.9 |
| ZnSO _{4(aq)} -stem Plant1 | 35 ± 2 | | 30 ± 2 | 35 ± 1 | | 0.8 |
| ZnSO _{4(aq)} -stem Plant2 | 29 ± 2 | | 35 ± 1 | 36 ± 1 | | 0.4 |
| ZnSO _{4(aq)} -stem Plant3 | 21 ± 2 | | 55 ± 1 | 24 ± 1 | | 0.7 |

^aThe linear combination fitting disagreement expressed as “R-factor” is the squared sum over all mismatch within the selected region between -20 and 50 eV relatively to edge. The formula is given in supplementary material.

Conversely, Fig. S6B-D shows that the intensity for K, Ca and Fe at stem irradiated by the handheld equipment randomly oscillated during the Zn kinetic monitoring. Therefore, our results did not show any evidence of radiation damage while monitoring the content of Zn in the stem.

It is also noteworthy that we did not observe any spectral changes during the acquisition of XANES for Zn organic reference compounds such as Zn-citrate, Zn-malate, or Zn-histidine (Fig. 6). This factor also points out that the monochromatic beam unlikely modified the chemical environment during the exposure time course. Thus, it seems that bending magnet beamlines at second-generation synchrotron facilities

may offer a good compromise for the *in vivo* and *in situ* analysis of biological samples since their X-ray brilliance is above laboratory XAS equipment, but below the high flux given by 3rd and 4th generation machines [39].

Two out of three plants exposed to ZnSO_{4(aq)} presented smaller XANES whiteline than those treated with Zn-EDTA (Fig. 6). At first glance, we suspected that this attenuation could be a distortion caused by incident beam self-absorption (IBSA). The IBSA happens when the sample is measured in fluorescence geometry and the concentration of the analyte affects the X-ray beam penetration depth. The consequence is the introduction of an artifact that dumps the amplitude of X-ray

absorption fine structure. However, the concentration of Zn at the speciation spot was $721 \pm 168 \text{ mg kg}^{-1}$ (determined by emission-transmission XRF). Usually, we have observed ISBA spectral distortions (compared to transmission measured spectra) in plant tissue samples which metal target concentration exceed $2000 - 2500 \text{ mg kg}^{-1}$.

The analysis of XANES spectra recorded at the stem of soybean (Figs. 5 and 6) allows stating that regardless of the source, the Zn was biotransformed in its way up to the shoot. The chemical species found in the present study partially agree with reports in the literature [16,22,40]. The dependency between Zn components and Zn source presented in Table 2 was also reported by Doolette et al. [16] who applied Zn-EDTA_(aq) and ZnSO_{4(aq)} to the leaves of *Triticum aestivum*. They found that the Zn components used in LCF (Zn-EDTA, Zn-phytate, Zn-cysteine, Zn-phosphate, Zn-citrate, and Zn-polygalacturonate) depend on the Zn source applied to leaves. Additionally, they showed that the weigh fractions of Zn presented spatial and concentration dependency.

Fig. 4 and Fig. 6 support the assumption of the coexistence of different forms of Zn. Zinc absorbed by roots is accumulated in the apoplast and symplast in three chemical forms: (1) exchangeable in the apoplast; (2) labile in the cytoplasm, and (3) non-labile, deposited in the vacuole and not translocated to the shoot [24]. In this study, Fig. 4 shows that Zn is simultaneously found in specialized transport tissues (major fraction) and cortex (minor fraction). Considering the energy of Zn K α emission (8.64 keV) and a 2 mm thick stem, the fraction of transmitted X-rays is around 20 %. It means that the region probed by XANES included the Zn present in both bundles (outer) and cortex (inner) tissues. Hence, in view of the number of components required to fit the spectra recorded in the stem, it is reasonable to assume that it could be under different chemical forms in each of these environments. This hypothesis shall be addressed in further studies using submicrometric X-ray beam, which may allow carrying out space-resolved chemical speciation in cross-sectioned stems.

Zinc complexed to phytate/phosphate is frequently reported in plant tissues. Zinc phytate/phosphate was found in leaves of *Triticum aestivum*, roots and shoot of *Zea mays* [14], and roots of *Eruca vesicaria* [41]. Additionally, positive spatial correlation between Zn and P was reported in *Triticum aestivum* grains [42]. However, we did not find any evidence of its presence in the stem of soybean. Phytates may represent 60–82 % of total P in several plant species [43], and the transition metal phytates complexes are mostly insoluble [44] as well as Zn phosphate ($K_{sp} = 9.1 \times 10^{-33}$) [45]. Zn-phytates are mostly found in seeds and roots of plants [46]. Due to the low solubility of the Zn-phytate, it is not expected to find in specialized transport tissues, such as the xylem. Terzano et al. [36] reported that Zn-phytate complex was mainly confined to the root endodermis of *Eruca vesicaria*, while in the xylem, Zn was found as Zn-citrate. Since Fig. 4 showed that Zn was mostly associated with transport than storage tissues, this might explain why neither phosphate nor phytate was necessary to adjust the XANES spectra recorded at the stem of soybean plants (Table 2).

The pH of xylem sap lies between 5–6.5, it contains nearly twice to three times more carboxylic acids than amino acids. The complexation is certainly a consequence of the chemical equilibrium resulted from the presence of metal ions and organic molecules (1–9 mM) [47,48]. Additionally, the complexation also ensures that the metal ions reach the target tissue either than precipitating in the way up.

The coexistence of a two-ring pattern and the accumulation of Zn in the epidermal region, as shown in Figs. 4 and S7, were previously reported for *Sedum alfredi* [49], *Phaseolus vulgaris* [19], and *Zea mays* [14]. Since there is no concentration gradient from the xylem to the epidermis, it is still not clear how Zn is loaded in the epidermal layer and how that image pattern is formed. In any case, the epidermal layer is supposed to act as storage tissue under high Zn concentration [19].

5. Conclusions

A fraction of Zn²⁺_(aq) supplied by ZnSO_{4(aq)} is chelated by EDTA_(aq) in the nutrient solution. The amount of Zn absorbed by the plant as defined in the root-solution interface, factors such as charge and diffusion coefficient might play significant roles. On the other hand, the Zn sources did not affect transport velocity in the stem. Besides, regardless of the source, the transport upwards seems to take place through the same pathway.

Zinc is neither transported as ZnSO_{4(aq)} nor as Zn-EDTA_(aq), but was biotransformed instead, reinforcing the chemical form in which Zn²⁺ is transported, slightly dependent on the content of the Zn²⁺ in the stem. Plants treated with Zn-EDTA exposed XANES spectra with higher whitelines than ZnSO_{4(aq)}. In the present study, the Zn concentration in the stem is the only measurable parameter that could explain this difference. It means that the type of complexes might depend on the concentration of Zn in the medium.

Authors contributions

G. S. Montanha, E. S. Rodrigues, and H. W. P. Carvalho performed the experiments and interpreted the results; E. Almeida assisted optimization of the XRF analysis and the writing of the manuscript; S. L. Z. Romeu assisted the writing of the manuscript; A.R. Reis assisted in the interpretation of the chemical speciation and the discussion of the manuscript; J. L. Jr. assisted in the discussion of the manuscript; G. S. Montanha, and H. W. P. Carvalho wrote the text; All authors read and approved the final version.

Declaration of Competing Interest

The authors declare that they have no known competing financial interests or personal relationships that could have appeared to influence the work reported in this paper.

Acknowledgments

The authors are grateful to LNLS for providing beamtime under proposal 2019-0015 and to Dr. S. Figueroa and J. M. Cintra for assistance during beamtime. We are grateful to A. Sant'Ana Neto for assistance during the Geochem chemical speciation.

Funding

This work was supported by the São Paulo Research Foundation grants 2015/05942-0, 2015/19121-8, 2017/16375-4, and FINEP project “Core Facility de suporte às pesquisas em Nutrologia e Segurança Alimentar na USP” grant number 01.12.0535.0. ARR and JLJ also thanks the National Council for Scientific and Technological Development (CNPq) for the research fellowship (grant 309380/2017-0 and #310572/2017-7, respectively).

Appendix A. Supplementary data

Supplementary material related to this article can be found, in the online version, at doi:<https://doi.org/10.1016/j.plantsci.2019.110370>.

References

- [1] B. Hafeez, Y.M. Khanif, M. Saleem, Role of zinc in plant nutrition- a review, *Am. J. Exp. Agric.* 3 (2013) 374–391.
- [2] D. Montalvo, F. Degryse, R.C. da Silva, R. Baird, M.J. McLaughlin, Agronomic effectiveness of zinc sources as micronutrient fertilizer, *Adv. Agron.* 139 (2016) 215–267.
- [3] N.K. Fageria, Níveis adequados e tóxicos de zinco na produção de arroz, feijão, milho, soja e trigo em solo de cerrado, *Rev. bras. eng. agríc. ambient.* 4 (2000) 390–395.

- [4] J.T. Sims, G.V. Johnson, Micronutrient soil tests, in: J.J. Mortvedt, F.R. Cox, L.M. Shuman, R.M. Welch (Eds.), *Micronutrients in Agriculture*, SSSA Book Series No. 4, Soil Science Society of America, Madison, 1991, pp. 427–476.
- [5] M. Sillanpää, *Micronutrients and the Nutrient Status of Soils: A Global Study*, FAO, Rome, 1982, pp. 1–444.
- [6] L.R.G. Guilherme, A.P. Corguinha, M. Sacco, M.D. Menezes, G.A. de Souza, Mapping zinc in soils from Brazil: spatial variability and factors influencing Zn availability, *Synergy in Science: Partnering for Solutions*, Annual Meeting, Nov. Minneapolis, 2015, pp. 15–18.
- [7] E.Z. Galvão, Correção da deficiência de zinco em lavouras de milho nos solos de cerrado, in: *Guia Técnico do Produtor Rural*, Embrapa, Distrito Federal (1999) 31.
- [8] A. Singh, Y.S. Shivay, Effect of summer green manuring crops and zinc fertilizer sources on productivity, Zn-uptake and economics of basmati rice, *J. Plant Nutr.* 39 (2016) 204–218.
- [9] Y. Arai, D.L. Sparks, Phosphate reaction dynamics in soils and soil components: a multiscale approach, in: D. Sparks (Ed.), *Advances in Agronomy*, Vol. 14, Academic Press, San Diego, 2007, pp. 135–179.
- [10] A. Zhao, S. Yang, B. Wang, X. Tian, Y. Zhang, Effects of ZnSO₄ and Zn-EDTA broadcast or banded to soil on Zn bioavailability in wheat (*Triticum aestivum* L.) and Zn fractions in soil, *Chemosphere* 205 (2018) 350–360.
- [11] P. Wang, D.M. Zhou, X.S. Luo, L.Z. Li, Effects of Zn-complexes on zinc uptake by wheat (*Triticum aestivum*) roots: a comprehensive consideration of physical, chemical and biological processes on biouptake, *Plant Soil* 316 (2009) 177–192.
- [12] B. Nowack, I. Schwyzer, R. Schulin, Uptake of Zn and Fe by wheat (*Triticum aestivum* var. Greina) and transfer to the grains in the presence of chelating agents (ethylenediaminedisuccinic acid and ethylenediaminetetraacetic acid), *J. Agric. Food Chem.* 56 (2008) 4643–4649.
- [13] P.C. Srivastava, D. Ghosh, V.P. Singh, Evaluation of different zinc sources for lowland rice production, *Biol. Fertil. Soils* 30 (1999) 168–172.
- [14] J. Lv, S. Zhang, L. Luo, J. Zhang, K. Yang, P. Christied, Accumulation, speciation and uptake pathway of ZnO nanoparticles in maize, *Environ. Sci. Nano* 2 (2015) 68–77.
- [15] R. Reid, J. Brookes, M. Tester, F.A. Smith, The mechanism of zinc uptake in plants, *Planta* 198 (2004) 39–45.
- [16] C.L. Doolette, T.L. Read, C. Li, K.G. Scheckel, E. Donner, P.M. Kopitke, J.K. Schjoerring, E. Lombi, Foliar application of zinc sulphate and zinc EDTA to wheat leaves: differences in mobility, distribution, and speciation, *J. Exp. Bot.* 69 (2018) 4469–4481.
- [17] M. Haschke, *Laboratory Micro-X-Ray Fluorescence Spectroscopy - Instrumentation and Applications*, Springer, Cham, 2014, pp. 1–356.
- [18] E.S. Rodrigues, M.H.F. Gomes, N.M. Duran, J.G.B. Cassanji, T.N.M. da Cruz, A. Sant'Anna Neto, S.M. Savassa, E. de Almeida, H.W.P. Carvalho, Laboratory microprobe X-ray fluorescence in plant science: emerging applications and case studies, *Front. Plant Sci.* 9 (2018) 1588.
- [19] T.N.M. da Cruz, S.M. Savassa, M.H.F. Gomes, E.S. Rodrigues, N.M. Duran, E. de Almeida, A.P. Martinelli, H.W.P. de Carvalho, Shedding light on the mechanisms of absorption and transport of ZnO nanoparticles by plants via in vivo X-ray spectroscopy, *Environ. Sci. Nano* 4 (2017) 2367–2376.
- [20] S.M. Savassa, N.M. Duran, E.S. Rodrigues, E. de Almeida, C.A.M. van Gestel, T.F.V. Bompadre, H.W.P. de Carvalho, Effects of ZnO nanoparticles on *Phaseolus vulgaris* germination and seedling development determined by X-ray spectroscopy, *ACS Appl. Nano Mater.* 1 (2018) 6414–6426.
- [21] N.K. Fageria, M.P. Barbosa Filho, A.B. Santos, Growth and zinc uptake and use efficiency in food crops, *Commun. Soil Sci. Plant Anal.* 39 (2008) 2258–2269.
- [22] J.A. Hernandez-Viezas, H. Castillo-Michel, J.C. Andrews, M. Cotte, C. Rico, J.R. Peralta-Videa, Y. Ge, J.H. Priester, P.A. Holden, J.L. Gardea-Torresdey, *In situ* synchrotron X-ray fluorescence mapping and speciation of CeO₂ and ZnO nanoparticles in soil cultivated soybean (*Glycine max*), *ACS Nano* 7 (2013) 1415–1423.
- [23] Monsoy, M7739 IPRO. http://www.monsoy.com.br/variedades_2_monsoy/m7739-ipro/ (accessed 19 June 2019).
- [24] J.E. Shaff, B.A. Schultz, E.J. Craft, R.T. Clark, L.V. Kochian, GEOCHEM-EZ: a chemical speciation program with greater power and flexibility, *Plant Soil* 330 (2010) 207–214.
- [25] H.A. Castillo-Michel, C. Larue, A.E. Pradas del Real, M. Cotte, G. Sarret, Practical review on the use of synchrotron based micro- and nano- X-ray fluorescence mapping and X-ray absorption spectroscopy to investigate the interactions between plants and engineered nanomaterials, *Plant Physiol. Biochem.* 110 (2017) 13–32.
- [26] G.L. Bovenkamp, *X-ray Absorption Spectroscopy in Biological Systems Opportunities and Limitations, Germany, 2013*, http://inis.iaea.org/search/search.aspx?orig_q=RN:44086523.
- [27] S.J.A. Figueroa, J.C. Mauricio, J. Murari, D.B. Beniz, J.R. Piton, H.H. Slepicka, M.F. De Sousa, A.M. Espíndola, A.P.S. Levinsky, Upgrades to the XAFS2 beamline control system and to the endstation at the LNLS, *J. Phys. Conf. Ser.* 712 (2016) 012022.
- [28] B. Ravel, M. Newville, ATHENA, ARTEMIS, HEPHAESTUS: data analysis for X-ray absorption spectroscopy using IFEFFIT, *J. Synchrotron Radiat.* 12 (2005) 537–541.
- [29] A. Moreira, L.A.C. Moraes, A.R. dos Reis, The molecular genetics of zinc uptake and utilization efficiency in crop plants, *Plant Micronutr. Use Effic.* (2018) 87–108.
- [30] B. Sattelmacher, The apoplast and its significance for plant mineral nutrition, *New Phytol.* 149 (2001) 167–192.
- [31] P.J. White, S.N. Whiting, A.J.M. Baker, M.R. Broadley, Does zinc move apoplastically to the xylem in roots of *Thlaspi caerulescens*? *New Phytol.* 153 (2002) 201–207.
- [32] M.J. Priest, N. America, *Pisolithus*— death of the pan-global super fungus, *New Phytol.* 153 (2002) 199–211.
- [33] C. Leifert, K.P. Murphy, P.J. Lumsden, Mineral and carbohydrate nutrition of plant cell and tissue cultures, *CRC Crit. Rev. Plant Sci.* 14 (1995) 83–109.
- [34] M.K. Sinha, B. Prasad, Effect of chelating agents on the kinetics of diffusion of zinc to a simulated root system and its uptake by wheat, *Plant Soil* 48 (1977) 599–612.
- [35] S. Oh, W.S. Shin, Separation of heavy metals from metal-EDTA in spent soil washing solution by using Na₂S, *J. Soil Groundw. Environ.* 20 (2015) 103–111.
- [36] R. Reid, J. Hayes, Mechanisms and control of nutrient uptake in plants, *Int. Rev. Cytol.* 229 (2003) 73–114.
- [37] G.L. Brattbauer, Preparation of frozen sections for analysis, in: C. Oliver, M. Jamur (Eds.), *Immunocytochemical Methods and Protocols*, Vol. 588, Humana Press, Totowa, 2010, pp. 67–73.
- [38] K.G. Scheckel, E. Lombi, S.A. Rock, M.J. McLaughlin, *In vivo* synchrotron study of thallium speciation and compartmentation in *Iberis intermedia*, *Environ. Sci. Technol.* 38 (2004) 5095–5100.
- [39] J.R. Helliwell, Synchrotron radiation facilities, *Nat. Struct. Biol.* 5 (1998) 614–617.
- [40] C. Li, P. Wang, A. Van Der Ent, M. Cheng, H. Jiang, T.L. Read, E. Lombi, C. Tang, M.D. De Jonge, N.W. Menzies, P.M. Kopitke, Absorption of foliar-applied Zn in sunflower (*Helianthus annuus*): importance of the cuticle, stomata and trichomes, *Ann. Bot.* 123 (2019) 57–68.
- [41] R. Terzano, Z. Al Chami, B. Vekemans, K. Janssens, T. Miano, P. Ruggiero, Zinc distribution and speciation within rocket plants (*Eruca vesicaria* L. Cavalieri) grown on a polluted soil amended with compost as determined by XRF microtomography and micro-XANES, *J. Agric. Food Chem.* 56 (2008) 3222–3231.
- [42] N. De Brier, S.V. Gomand, E. Donner, D. Paterson, E. Smolders, J.A. Delcour, E. Lombi, Element distribution and iron speciation in mature wheat grains (*Triticum aestivum* L.) using synchrotron X-ray fluorescence microscopy mapping and X-ray absorption near-edge structure (XANES) imaging, *Plant Cell Environ.* 39 (2016) 1835–1847.
- [43] V. Ravindran, G. Ravindran, S. Sivalogan, Total and phytate phosphorus contents of various foods and feedstuffs of plant origin, *Food Chem.* 50 (1994) 133–136.
- [44] C.J. Wyatt, A. Triana-Tejas, Soluble and insoluble Fe, Zn, Ca, and phytates in foods commonly consumed in northern Mexico, *J. Agric. Food Chem.* 42 (1994) 2204–2209.
- [45] K.W. Whitten, R.E. Davis, M.L. Peck, G.G. Stanley, *Chemistry*, Thomson Brooks/Cole, Belmont, 2007.
- [46] D. Oberleas, The role of phytate in zinc bioavailability and homeostasis, in: G.E. Inglett (Ed.), *Nutritional Bioavailability of Zinc*, American Chemical Society, Washington, 1983, pp. 145–158.
- [47] M.C. White, F.D. Baker, R.L. Chaney, A.M. Decker, Metal complexation in xylem fluid, *Plant Physiol.* 67 (1981) 301–310.
- [48] A. Kutrowska, M. Szlag, Low-molecular weight organic acids and peptides involved in the long-distance transport of trace metals, *Acta Physiol. Plant.* 36 (2014) 1957–1968.
- [49] S.K. Tian, L.L. Lu, X.E. Yang, J.M. Labavitch, Y.Y. Huang, P. Brown, Stem and leaf sequestration of zinc at the cellular level in the hyperaccumulator *Sedum alfredii*, *New Phytol.* 182 (2009) 116–126.